PERGAMON

International Journal of Solids and Structures 38 (2001) 5581–5594

INTERNATIONAL JOURNAL OF SOLIDS and STRUCTURES

www.elsevier.com/locate/ijsolstr

Theoretical models for void coalescence in porous ductile solids. I. Coalescence "in layers"

Mihai Gologanu [a], Jean-Baptiste Leblond [a,*], Gilles Perrin [b], Josette Devaux [c]

[a] *Laboratoire de Modélisation en Mécanique, Université Pierre et Marie Curie, 8 rue du Capitaine Scott, 75015 Paris, France*
[b] *Institut Français du Pétrole, Division de Mécanique Appliquée, 1-4 avenue de Bois-Préau, 92852 Rueil-Malmaison Cedex, France*
[c] *SYSTUS International, 84 boulevard Vivier-Merle, 69485 Lyon Cedex 03, France*

Received 3 May 2000

Abstract

This paper and its companion address the problem of theoretically predicting coalescence of cavities in periodically voided ductile solids. One considers, as in several previous finite element (FE) studies, a cylindrical representative volume element (RVE) containing an initially spheroidal void and subjected to some axisymmetric loading. We consider here the case where the major stress applied is the axial one so that the strain is mainly vertical. As a consequence, voids gradually concentrate in horizontal bands. Coalescence corresponds to a sudden concentration of the deformation in these regions. In the model, one considers the RVE as made up of three layers, a highly porous one containing the void surrounded by two sound ones; the strain rate and stress fields are considered as homogeneous in each region. A recent model proposed by the authors, analogous to that of Gurson but accounting for void shape, is used to describe the behavior of the central layer while the outer ones obey von Mises' criterion. Two regimes are possible according to whether the sound zones are plastic or rigid; the first one corresponds to the pre-coalescence period while the second one corresponds to coalescence. The simple model thus obtained is entirely analytic. Comparisons with various FE simulations are presented for several initial porosities, void shapes and triaxialities, and the predictions of the model are found to agree quite well with the numerical results. © 2001 Elsevier Science Ltd. All rights reserved.

Keywords: Ductile fracture; Void coalescence; Periodic medium; Void shape effects; Predictive model; Numerical simulations

1. Introduction

Micromechanical finite element (FE) analyses of void growth and coalescence in periodically voided ductile solids were initiated by the pioneering work of Koplik and Needleman (1988). As in several subsequent works (among which those of Brocks et al. (1995), Sovik (1996), Pardoen and Delannay (1998)), the authors considered an initially spherical or spheroidal void embedded in an axisymmetric cylindrical "cell". This geometry was in fact an approximation of a cylindrical volume with some hexagonal basis, which can be considered as an elementary cell in a periodically voided material. Fully three-dimensional

* Corresponding author. Tel.: +33-1-44-27-39-24; fax: +33-1-44-27-52-59.
E-mail address: leblond@lmm.jussieu.fr (J.-B. Leblond).

0020-7683/01/$ - see front matter © 2001 Elsevier Science Ltd. All rights reserved.
PII: S0020-7683(00)00354-1

computations were also performed by Hom and McMeeking (1989), Worswick and Pick (1990), Richelsen and Tvergaard (1994) and Kuna and Sun (1996).

In most of these works, and especially in all two-dimensional simulations, the elementary cell was subjected to an axisymmetric loading ($\Sigma_{xx} = \Sigma_{yy} \neq 0$, $\Sigma_{zz} \neq 0$, other $\Sigma_{ij} = 0$, where z denotes the direction of the axis of symmetry), with a major axial stress ($\Sigma_{zz} > \Sigma_{xx}$). In this case, due to axial stretching and radial contraction, the vertical distance between neighboring voids gradually becomes larger than the horizontal one, even if these distances were initially equal (as generally assumed). The resulting void distribution therefore becomes more and more anisotropic. Onset of coalescence corresponds to some instant when the strain rate suddenly localizes (in a diffuse manner) in the horizontal inter-void ligaments, the other zones of the material becoming rigid. The presence of these horizontal rigid zones precludes any further horizontal contraction so that the deformation mode suddenly becomes a uniaxial, vertical stretching. This phenomenon will be termed "coalescence in layers" in this paper. (A different type of coalescence, "in columns", will be considered in Part II.)

Theoretical modeling of coalescence in layers started with the early, seminal work of Thomason (1985). Using limit analysis, this author proposed an approximate formula for the "critical" axial stress inducing some plastic flow localized in the horizontal ligament between neighboring voids. This provided a criterion for coalescence of voids, which could indeed be considered to occur when the actual value of the axial stress reached its "critical" value. Another approach was proposed by Perrin (1992). He accounted for the strain-induced anisotropy of the void distribution by schematizing the axisymmetric cylindrical cell considered as made up of three horizontal layers, a highly porous central one (containing the void) surrounded by two sound ones, the strain rate and stresses being homogeneous in each zone. Gurson (1977) famous model for porous plastic solids containing spherical voids was used to describe the behavior of the porous zone, and coalescence was considered to occur when Rudnicki and Rice's (1975) well-known criterion for strain localization, as applied to Gurson's model by Yamamoto (1978), was met in this zone. Very recently, Pardoen and Hutchinson (2000) combined extension of Gologanu et al. (1997) of Gurson's model incorporating void shape effects with Thomason's (1985) approach to model coalescence even under relatively low (<1) triaxialities, for which such shape effects become important. Essentially the same approach was even more recently followed by Benzerga (2000), the main difference being a somewhat different treatment of the overall behavior after the onset of coalescence.

All of these models provided acceptable predictions concerning coalescence in periodically voided solids, as evidenced by comparisons with results of FE micromechanical simulations. It is the purpose of this paper, however, to show that they can nevertheless be further improved. The improvements will be threefold. First, and most importantly, the agreement between the model predictions and the numerical results will be better, at least for low [1] triaxialities. Second, from a conceptual viewpoint, the model will be more "economical" in the sense that the pre-coalescence and coalescence periods will be treated in a simple, unified way, without appealing to any special "coalescence criterion" such as Rudnicki and Rice's (1975) localization condition in Perrin's (1992) work and Thomason's (1985) criterion in those of Pardoen and Hutchinson (2000) and Benzerga (2000). Finally, the model developed will be more versatile in that it will more easily be extended to the case of coalescence "in columns", as will be shown in Part II, and to coalescence in porous *viscoplastic* materials, as will be expounded in a future paper.

The model to be developed is inspired from that of Perrin (1992) in that we shall retain one of its essential features, namely the schematization of the axisymmetric cylindrical cell as a "sandwich" made up of three layers (sound, highly porous, sound) in which the strain rate and stress fields are considered as homogeneous. However, there will be several differences. The first one will be that just as in the recent works of Pardoen and Hutchinson (2000) and Benzerga (2000), in order to account for void shape effects, we shall

[1] But not too low, otherwise coalescence does not occur.

use extension of Gologanu et al. (1997) of Gurson (1977) original model rather than that model itself. The second difference is more subtle and connected to a remark made by Suquet (private communication, 1992) about Perrin's (1992) work, but which in fact applies to all previous coalescence models. Suquet indeed noted that since Perrin (1992) described the overall behavior of the unit cell, prior to coalescence, through application of Gurson (1977) model to the *entire cell*, not the central, highly porous layer, he did not account for the strain-induced anisotropy of the void distribution *prior to coalescence*. In contrast, we shall consider the cell as made up of three layers (applying extension of Gologanu et al. (1997) Gurson (1977) model to the central one) *right from the beginning of the loading*, thus accounting for this anisotropy already before the onset of coalescence. It will be seen that this is the key to improving the model predictions at low triaxialities. A third difference with respect to Perrin's (1992) approach will be that we shall abandon Rudnicki and Rice's (1975) theory of strain localization to predict onset of coalescence. Instead, coalescence will emerge in a natural way from the model, as corresponding to a transition from a phase where the three layers are all plastic, to another phase where the sound ones become rigid. Finally, unlike in Perrin's (1992) work, no additional element [2] will be introduced to describe the coalescence phase, which will simply correspond, as just stated, to the period when the sound layers are no longer plastic but rigid.

The paper is organized as follows. We first recall in Section 2 the elements of Gologanu et al. (1997) model for porous ductile solids containing spheroidal voids, considering only axisymmetric loadings aligned with the axis of the voids for the sake of simplicity (which is sufficient for the present purposes). Next, in Section 3, we expound the equations of our model of coalescence in layers, distinguishing between the pre-coalescence and coalescence phases. Section 4 is finally devoted to comparisons with the results of micromechanical simulations, either taken from the literature (Koplik and Needleman, 1988; Sovik, 1996) or new.

2. The GLD model for porous ductile solids containing spheroidal voids

2.1. Generalities

We begin by recalling the elements of the model proposed by Gologanu et al. (1997) and Gologanu et al. (1997) (hereafter referred to as the Gologanu-Leblond-Devaux (GLD) model) in order to introduce void shape effects in a Gurson-like description of porous plastic materials. The sound (void-free) matrix will be assumed to be (rigid) ideal plastic, with yield stress σ_0 in uniaxial tension. Indeed, since various authors have shown that strain hardening has only a weak influence upon coalescence, we shall disregard it in the present paper. Also, we shall give the equations of the GLD model only for axisymmetric loadings aligned with the axis z of the voids ($\Sigma_{xx} = \Sigma_{yy} \neq 0$, $\Sigma_{zz} \neq 0$, other $\Sigma_{ij} = 0$), since coalescence will be considered only for such loadings.

The GLD model is based on the consideration of some RVE of spheroidal shape containing a *confocal* spheroidal void (Fig. 1). The void and the RVE can be either prolate (Fig. 1a) or oblate (Fig. 1b). These two cases will be referred to through the symbols (P) and (O), respectively, in the equations to follow. The semi-axis of the void along the vertical direction is denoted a_1, and that along the horizontal ones, b_1. The semi-axes of the RVE are similarly denoted a_2 and b_2. Because of confocality, these semi-axes are related by the relation $\sqrt{|a_1^2 - b_1^2|} = \sqrt{|a_2^2 - b_2^2|} \equiv c$ where c denotes the focal distance. Such a geometry can be characterized, up to some unimportant homothetical transformation, by two dimensionless parameters, the porosity f and the shape parameter S of the void, defined by

$$f \equiv \frac{a_1 b_1^2}{a_2 b_2^2}, \qquad S \equiv \ell n \frac{a_1}{b_1}. \tag{1}$$

[2] Except for a slightly modified evolution equation for the void shape parameter.

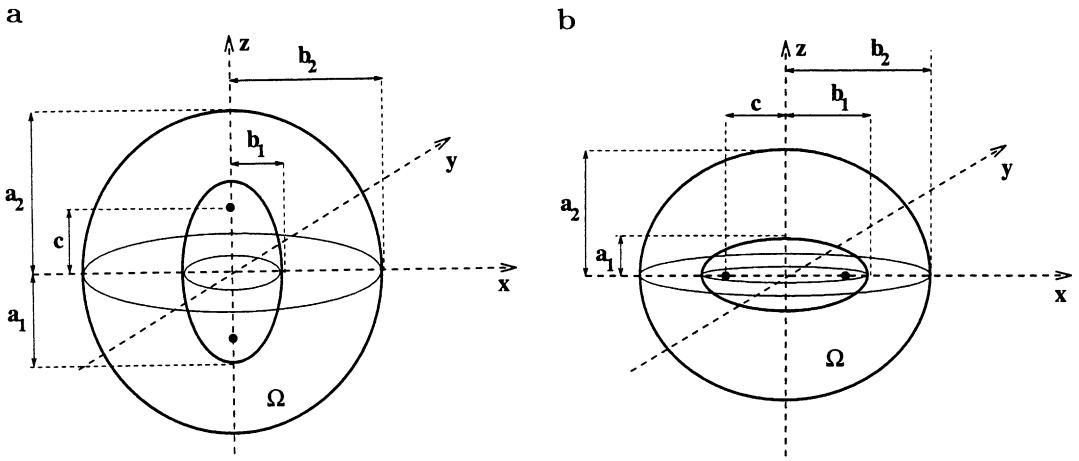

Fig. 1. The RVE considered in the GLD model: (a) prolate void, and (b) oblate void.

With this definition, S varies from 0 to $+\infty$ for prolate voids and from 0 to $-\infty$ for oblate ones. Use will also be made of the inner and outer eccentricities $e_1 \equiv c/a_1$ (P) or c/b_1 (O), $e_2 \equiv c/a_2$ (P) or c/b_2 (O). It is easy to check that these quantities are connected to the parameters f and S by the following formulae:

$$1 - e_1^2 = \exp(-2 \mid S \mid), \qquad \begin{cases} f\frac{1-e_2^2}{e_2^3} = \frac{1-e_1^2}{e_1^3} \ \text{(P)}, \\ f\frac{\sqrt{1-e_2^2}}{e_2^3} = \frac{\sqrt{1-e_1^2}}{e_1^3} \ \text{(O)}. \end{cases} \tag{2}$$

2.2. Yield criterion

The GLD criterion is of the form, for axisymmetric loadings:

$$\frac{C}{\sigma_0^2}(\Sigma_{zz} - \Sigma_{xx} + \eta\Sigma_h)^2 + 2q(g+1)(g+f)\cosh\left(\kappa\frac{\Sigma_h}{\sigma_0}\right) - (g+1)^2 - q^2(g+f)^2 = 0, \tag{3}$$

$$\Sigma_h \equiv 2\alpha_2\Sigma_{xx} + (1-2\alpha_2)\Sigma_{zz}. \tag{4}$$

In these expressions the parameters g (the "second porosity"), κ and α_2 are given by

$$g = \begin{cases} 0 & \text{(P)}, \\ \frac{e_2^3}{\sqrt{1-e_2^2}} & \text{(O)}, \end{cases} \tag{5}$$

$$\kappa^{-1} = \begin{cases} \frac{1}{\sqrt{3}} + \frac{1}{\ell\mathrm{n}\, f}\left((\sqrt{3}-2)\ell\mathrm{n}\frac{e_1}{e_2} - \frac{1}{\sqrt{3}}\ell\mathrm{n}\frac{3+e_1^2+2\sqrt{3+e_1^4}}{3+e_2^2+2\sqrt{3+e_2^4}} + \ell\mathrm{n}\frac{\sqrt{3}+\sqrt{3+e_1^4}}{\sqrt{3}+\sqrt{3+e_2^4}}\right) \ \text{(P)}, \\ \frac{2}{3} + \frac{\frac{2}{3}(g_f-g_1)+\frac{2}{5}(g_f^{5/2}-g_1^{5/2})(\frac{4}{3}-g_f^{5/2}-g_1^{5/2})}{\ell\mathrm{n}(g_f/g_1)}, \quad g_f \equiv \frac{g}{g+f}, \quad g_1 \equiv \frac{g}{g+1} \ \text{(O)}, \end{cases} \tag{6}$$

$$\alpha_2 = \begin{cases} \frac{1+e_2^2}{3+e_2^4} \ \text{(P)}, \\ \frac{(1-e_2^2)(1-2e_2^2)}{3-6e_2^2+4e_2^4} \ \text{(O)}. \end{cases} \tag{7}$$

Also, the quantities η and C are given by

$$\eta = -\frac{Q\kappa(g+1)(g+f)\mathrm{sh}}{(g+1)^2+(g+f)^2+(g+1)(g+f)(\kappa H\,\mathrm{sh}-2\,\mathrm{ch})}, \tag{8}$$

$$C = -\frac{\kappa(g+1)(g+f)\mathrm{sh}}{(Q+\eta H)\eta}, \tag{9}$$

where

$$\mathrm{sh}\equiv\sinh(\kappa H),\quad \mathrm{ch}\equiv\cosh(\kappa H),\quad H=2(\alpha_1-\alpha_2),\quad Q=1-f, \tag{10}$$

the parameter α_1 being itself given by

$$\alpha_1=\begin{cases}\frac{1}{2e_1^2}-\frac{1-e_1^2}{2e_1^3}\,\mathrm{arg\,tanh}\,e_1\ (\mathrm{P}),\\ -\frac{1-e_1^2}{2e_1^2}+\frac{\sqrt{1-e_1^2}}{2e_1^3}\,\mathrm{arc\,sin}\,e_1\ (\mathrm{O}).\end{cases} \tag{11}$$

Finally, q is the analog of the heuristic parameter q_1 introduced by Tvergaard's (1981) in Gurson (1977) criterion (for spherical voids), which is considered to depend upon the void shape according to the formula

$$q = 1+2(q_0-1)\frac{e^S}{1+e^{2S}}\ , \tag{12}$$

where q_0 denotes the value of q for spherical cavities ($S=0$).

2.3. Flow rule

It has been shown by Gurson (1977) that for metallic materials, which obey the normality property on a microscopic scale, such a property is also satisfied at the macroscopic scale of "homogenized" models. It follows that the flow rule is given by

$$\begin{cases} D_{xx}=H\left[\frac{C}{\sigma_0^2}(2\eta\alpha_2-1)(\Sigma_{zz}-\Sigma_{xx}+\eta\Sigma_h)+2\alpha_2 q(g+1)(g+f)\frac{\kappa}{\sigma_0}\sinh\left(\kappa\frac{\Sigma_h}{\sigma_0}\right)\right],\\ D_{zz}=2H\left[\frac{C}{\sigma_0^2}(1+\eta(1-2\alpha_2))(\Sigma_{zz}-\Sigma_{xx}+\eta\Sigma_h)+(1-2\alpha_2)q(g+1)(g+f)\frac{\kappa}{\sigma_0}\sinh\left(\kappa\frac{\Sigma_h}{\sigma_0}\right)\right],\end{cases} \tag{13}$$

where $H\ (\geqslant 0)$ denotes the plastic multiplier. Note that a factor of 2 is apparently missing in the first term of Eq. (13) for D_{xx}. The explanation is that one must write Σ_{xx} as $(\Sigma_{xx}+\Sigma_{yy})/2$ and consider Σ_{xx} and Σ_{yy} as distinct when evaluating the derivative of the yield function (given by Eq. (3)) with respect to Σ_{xx}.

2.4. Evolution equations for the porosity and the void shape parameter

The evolution equation for f is the usual one, deduced from incompressibility of the sound matrix:

$$\dot f = (1-f)\mathrm{tr}\,\mathbf{D}. \tag{14}$$

The evolution equation for S reads

$$\dot S = h(D_{zz}-D_{xx})+\left(\frac{1-3\alpha_1}{f}+3\alpha_2-1\right)\mathrm{tr}\,\mathbf{D}. \tag{15}$$

The parameter h in this equation is of semi-heuristic origin; it is given by

$$h = 1+\frac{9}{2}h_T\left(1-\sqrt{f}\right)^2\frac{\alpha_1-\alpha_1'}{1-3\alpha_1}. \tag{16}$$

The expression of the parameter α_1' in Eq. (16), which was first encountered in the work of Garajeu (1995), is as follows:

$$\alpha_1' = \begin{cases} \frac{1}{3-e_1^2} & \text{(P)}, \\ \frac{1-e_1^2}{3-2e_1^2} & \text{(O)}. \end{cases} \tag{17}$$

Also, the heuristic parameter h_T, which depends upon the triaxiality

$$T \equiv \frac{\frac{1}{3}(2\Sigma_{xx} + \Sigma_{zz})}{|\Sigma_{zz} - \Sigma_{xx}|}, \tag{18}$$

is given by

$$h_T = \begin{cases} 1 - T^2 & \text{if } (\Sigma_{zz} - \Sigma_{xx})\text{tr } \mathbf{\Sigma} > 0, \\ 1 - T^2/2 & \text{if } (\Sigma_{zz} - \Sigma_{xx})\text{tr } \mathbf{\Sigma} < 0. \end{cases} \tag{19}$$

Note that the expression of h_T is somewhat different from that proposed by Gologanu et al. (1997). The origin of the difference is discussed in detail in Gologanu's (1997) thesis and briefly recalled in Appendix A.

3. Model for coalescence in layers

3.1. Generalities

We consider, just as in most numerical studies, a cylindrical RVE containing an initially spherical or spheroidal void. The shape of the void is considered to remain spheroidal during the whole mechanical history. (In fact, this becomes wrong during coalescence, but the modified evolution equation for S given below is precisely designed to account for this.) The dimensions of the void are denoted a and b, and those of the cylinder, A and B (Fig. 2a). The RVE is subjected to some "macroscopic" axisymmetric ($\Sigma_{xx} = \Sigma_{yy}$) tensile (tr $\mathbf{\Sigma} > 0$) loading, the upper and lower surfaces remaining planar and the lateral one cylindrical. The major principal stress is assumed to be the axial one: $\Sigma_{zz} > \Sigma_{xx}$. The triaxiality T (defined by Eq. (18)) is assumed to be fixed during the whole mechanical history.

As explained in Section 1, for such a loading, coalescence will occur "in layers": due to axial stretching and lateral contraction, the vertical void spacing will increase and the horizontal one decrease, resulting in a

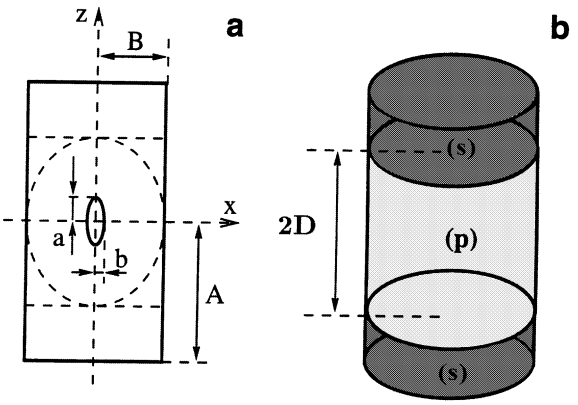

Fig. 2. The RVE considered in the model for coalescence in layers: (a) real RVE, and (b) model composite structure.

strain-induced anisotropy of the void distribution; onset of coalescence will occur when the strain rate suddenly concentrates in the horizontal ligaments separating voids, the remaining parts of the material becoming then rigid. Following Perrin's (1992) idea, we account for this strain-induced anisotropy of the void distribution by schematizing the RVE as made up of three horizontal layers (Fig. 2b). The central one, of thickness $2D$, is highly porous, while the surrounding ones, of thickness $A-D$, are fully sound. The stress and strain rate fields are considered as homogeneous in each zone. The GLD model, accounting for void shape effects, is employed to describe the behavior of the central layer, while the surrounding ones are assumed to obey von Mises' criterion and the associated flow rule.

The schematization adopted immediately raises the problem of the choice of the thickness $2D$ of the central zone. Ours is based on the consideration that since the behavior of this portion of cylinder is to be described by the GLD model, it should be geometrically as close as possible to the RVE used for the derivation of that model, namely a spheroid confocal with the void. This leads to the "confocality condition"

$$D^2 - B^2 = a^2 - b^2 \quad \Rightarrow \quad D = \sqrt{B^2 + a^2 - b^2}. \tag{20}$$

Note that for a spherical cavity ($a = b$), second term of formula (20) reduces to $D = B$, which was the choice proposed by Perrin (1992) from a somewhat different argument.

Second term of formula (20) for D was very recently criticized by Benzerga (2000) on the following grounds. Since the sound layers are to become rigid during the coalescence phase, they should correspond to those rigid zones effectively observed in FE simulations. Now it is found in such simulations that these zones extend down to, or up to, the poles of the void. This favors the choice $D = a$, rather than $D = \sqrt{B^2 + a^2 - b^2}$.

Benzerga's argument is indeed compelling for the coalescence phase. However, our choice for D is more logical prior to coalescence, for the reason expounded above. Also, it has been shown by Gologanu et al. (1997) that the two possible definitions for D in fact lead in practice to rather similar values. Finally, it will be shown below that our choice allows for quite satisfactory predictions of the onset and development of coalescence.

We denote by p the volume proportion of the central porous layer within the RVE and by $f^{(\mathrm{p})} \equiv 2ab^2/(3DB^2)$ the porosity in that layer; thus

$$p = \frac{D}{A}, \qquad f^{(\mathrm{p})} = \frac{f}{p}, \tag{21}$$

where $f \equiv 2ab^2/(3AB^2)$ denotes the porosity in the whole RVE. More generally, we shall use an upper index (p) to denote quantities defined in the central porous layer and an index (s) for those defined in the sound ones (for instance $\Sigma_{xx}^{(\mathrm{p})}$, $\Sigma_{xx}^{(\mathrm{s})}$, $D_{zz}^{(\mathrm{p})}$, $D_{zz}^{(\mathrm{s})}$), whenever necessary. However, we shall drop these indices when superfluous, that is for quantities defined only either in the porous layer or the sound ones (such as the shape parameter S or the "second porosity" g for instance, which "exist" only in the porous zone), or for those quantities which are identical in the different zones. For instance, because of axial equilibrium, the vertical stress is the same in all layers: $\Sigma_{zz}^{(\mathrm{p})} = \Sigma_{zz}^{(\mathrm{s})} \equiv \Sigma_{zz}$. Also, since the lateral surface is ascribed to remain cylindrical, the horizontal strain rate is uniform too: $D_{xx}^{(\mathrm{p})} = D_{xx}^{(\mathrm{s})} \equiv D_{xx}$.

3.2. Pre-coalescence phase

This phase corresponds to plastic flow of the entire RVE. Therefore the stresses $\Sigma_{xx}^{(\mathrm{s})}$, Σ_{zz} in the sound layers obey the von Mises criterion:

$$\Sigma_{zz} - \Sigma_{xx}^{(\mathrm{s})} = \sigma_0 \quad \Rightarrow \quad \Sigma_{xx}^{(\mathrm{s})} = \Sigma_{zz} - \sigma_0 \tag{22}$$

(it is assumed here that $\Sigma_{xx}^{(s)}$, just like Σ_{xx}, is smaller than Σ_{zz}). Furthermore the overall stress Σ_{xx} is obviously related to the stresses $\Sigma_{xx}^{(p)}$, $\Sigma_{xx}^{(s)}$ in the porous and sound layers by the relation

$$\Sigma_{xx} = p\Sigma_{xx}^{(p)} + (1-p)\Sigma_{xx}^{(s)} \quad \Rightarrow \quad \Sigma_{xx}^{(p)} = \frac{1}{p}\left[\Sigma_{xx} - (1-p)\Sigma_{xx}^{(s)}\right] = \frac{1}{p}\left[\Sigma_{xx} - (1-p)(\Sigma_{zz} - \sigma_0)\right] \tag{23}$$

(where Eq. (22) has been used). Finally, the overall stresses Σ_{xx}, Σ_{zz} are related by Eq. (18) with $\Sigma_{zz} > \Sigma_{xx}$, so that (by Eq. (23))

$$\Sigma_{xx} = \frac{3T-1}{3T+2}\Sigma_{zz} \quad \Rightarrow \quad \Sigma_{xx}^{(p)} = \frac{1}{p}\left[\left(\frac{3T-1}{3T+2} - 1 + p\right)\Sigma_{zz} + (1-p)\sigma_0\right]. \tag{24}$$

Thus all stress components can be calculated in terms of the sole unknown Σ_{zz}. This unknown can finally be deduced from the fact that the GLD criterion (Eqs. (3) and (4)) is met in the porous layer:

$$\begin{aligned} &\frac{C}{\sigma_0^2}(\Sigma_{zz} - \Sigma_{xx}^{(p)} + \eta\Sigma_h)^2 + 2q(g+1)(g+f^{(p)})\cosh\left(\kappa\frac{\Sigma_h}{\sigma_0}\right) - (g+1)^2 - q^2(g+f^{(p)})^2 = 0, \\ &\Sigma_h \equiv 2\alpha_2\Sigma_{xx}^{(p)} + (1-2\alpha_2)\Sigma_{zz}. \end{aligned} \tag{25}$$

In these expressions, the values of the parameters g, κ, α_2, η, C, q are given by the formulae of Section 2 (Eqs. (2) and (5)–(12)), except for the sole replacement of the "overall" porosity f by that, $f^{(p)}$, of the porous layer.

Once the stresses are known, the components D_{xx}, $D_{zz}^{(p)}$ of the strain rate in the porous layer can be deduced, up to some arbitrary positive multiplicative constant, from the flow rule (13) with the appropriate replacements:

$$\begin{aligned} D_{xx} &= H\left[\frac{C}{\sigma_0^2}(2\eta\alpha_2 - 1)(\Sigma_{zz} - \Sigma_{xx}^{(p)} + \eta\Sigma_h) + 2\alpha_2 q(g+1)(g+f^{(p)})\frac{\kappa}{\sigma_0}\sinh\left(\kappa\frac{\Sigma_h}{\sigma_0}\right)\right], \\ D_{zz}^{(p)} &= 2H\left[\frac{C}{\sigma_0^2}(1+\eta(1-2\alpha_2))(\Sigma_{zz} - \Sigma_{xx}^{(p)} + \eta\Sigma_h) + (1-2\alpha_2)q(g+1)(g+f^{(p)})\frac{\kappa}{\sigma_0}\sinh\left(\kappa\frac{\Sigma_h}{\sigma_0}\right)\right]. \end{aligned} \tag{26}$$

Furthermore, the component $D_{zz}^{(s)}$ of the strain rate in the sound layers is easily deduced from D_{xx} using incompressibility of these layers:

$$D_{zz}^{(s)} = -2D_{xx}. \tag{27}$$

Finally the component D_{zz} of the overall strain rate is obtained from the relation

$$D_{zz} = pD_{zz}^{(p)} + (1-p)D_{zz}^{(s)}. \tag{28}$$

The global strain rate $\mathbf{D}$ being known, the rate of the overall porosity f is given by the (unmodified) evolution equation (14) (which is recalled to be rigorous since it only results from incompressibility of the sound matrix). The strain rate $\mathbf{D}^{(p)}$ in the porous layer being also known, the evolution of the void shape parameter is deduced from Eq. (15), with the appropriate replacements:

$$\dot{S} = h\left(D_{zz}^{(p)} - D_{xx}\right) + \left(\frac{1-3\alpha_1}{f^{(p)}} + 3\alpha_2 - 1\right)\mathrm{tr}\,\mathbf{D}^{(p)}. \tag{29}$$

The parameter h in this equation is given by formulae (16), (17) and first term of Eq. (19), f being replaced by $f^{(p)}$ and the overall triaxiality $T \equiv \frac{1}{3}(2\Sigma_{xx} + \Sigma_{zz})/(\Sigma_{zz} - \Sigma_{xx})$ by that, $T^{(p)} \equiv \frac{1}{3}(2\Sigma_{xx}^{(p)} + \Sigma_{zz})/(\Sigma_{zz} - \Sigma_{xx}^{(p)})$, in the porous layer.

The above formulae allow for the step-by-step calculation of all quantities of interest (stresses, porosity, shape parameter of the void) as functions of some "control parameter". Any such parameter may be chosen; in practice we shall use, like other authors, the overall equivalent cumulated strain E_{eq} defined by

$$E_{\mathrm{eq}} \equiv \int_0^t \left(\frac{2}{3}\mathbf{D}' : \mathbf{D}'\right)^{1/2}(\tau)\,\mathrm{d}\tau = \int_0^t \frac{2}{3}(D_{zz} - D_{xx})(\tau)\,\mathrm{d}\tau, \tag{30}$$

where $\mathbf{D}'$ denotes the deviator of $\mathbf{D}$.

The pre-coalescence phase stops when D_{xx} (given by the first term of Eq. (26)) becomes zero.

3.3. Coalescence phase

During the coalescence phase, the porous layer is still plastic; hence Eq. (25) still hold. However, the sound layers now become rigid, so that $\Sigma_{xx}^{(\mathrm{p})}$ can no longer be expressed in terms of Σ_{zz} as in second term of Eq. (24), which was a consequence of the von Mises criterion's being met in these layers. However, precisely because of the rigidity of the sound zones, the strain rate D_{xx} is now zero. Hence the flow rule (26) in the porous layer implies that

$$\frac{C}{\sigma_0^2}(2\eta\alpha_2 - 1)(\Sigma_{zz} - \Sigma_{xx}^{(\mathrm{p})} + \eta\Sigma_h) + 2\alpha_2 q(g+1)(g + f^{(\mathrm{p})})\frac{\kappa}{\sigma_0}\sinh\left(\kappa\frac{\Sigma_h}{\sigma_0}\right) = 0. \tag{31}$$

Expressing $\Sigma_{zz} - \Sigma_{xx}^{(\mathrm{p})} + \eta\Sigma_h$ in terms of $\sinh(\kappa\Sigma_h/\sigma_0)$ using this equation and inserting the result into first term of Eq. (25), one gets the following algebraic second-degree equation on the unknown $\cosh(\kappa\Sigma_h/\sigma_0)$:

$$\frac{4\alpha_2^2 q^2 (g+1)^2 (g+f^{(\mathrm{p})})^2 \kappa^2}{C(1-2\eta\alpha_2)^2}\left[\cosh^2\left(\kappa\tfrac{\Sigma_h}{\sigma_0}\right) - 1\right] + 2q(g+1)(g+f^{(\mathrm{p})})\ \cosh\left(\kappa\tfrac{\Sigma_h}{\sigma_0}\right) - (g+1)^2 - q^2(g+f^{(\mathrm{p})})^2 = 0. \tag{32}$$

One must of course select the solution of this equation which is greater than unity. Assuming Σ_h to be positive like $\frac{1}{3}(\mathrm{tr}\,\boldsymbol{\Sigma})$, one deduces its value from there. Thus, by second term of Eq. (25), $2\alpha_2\Sigma_{xx}^{(\mathrm{p})} + (1-2\alpha_2)\Sigma_{zz}$ is known, and so is also $\Sigma_{zz} - \Sigma_{xx}^{(\mathrm{p})}$ by Eq. (31); the values of $\Sigma_{xx}^{(\mathrm{p})}$ and Σ_{zz} follow.

With regard to the strain rate, D_{xx} and $D_{zz}^{(\mathrm{s})}$ are zero since the sound layers are rigid; furthermore $D_{zz}^{(\mathrm{p})}$ and D_{zz} are connected through formula (28) (with $D_{zz}^{(\mathrm{s})} = 0$). Thus the various strain rate components are determined up to some arbitrary positive constant.

Once the strain rate is known, the porosity rate can again be deduced from Eq. (14). The rate of the void shape parameter is then given by the following equation:

$$\dot{S} = [\gamma(h + \frac{1-3\alpha_1}{f^{(\mathrm{p})}} + 3\alpha_2 - 1) + \frac{1}{2f^{(\mathrm{p})}}(\gamma - 2)]D_{zz}^{(\mathrm{p})}, \quad \gamma = 2/3. \tag{33}$$

This slightly modified (with respect to Eq. (29)) formula was proposed by Gologanu et al. (1997) in order to account for the quick evolution of the void toward more oblate shapes during coalescence (due to the lateral shrinkage of the inter-void ligament); it is of semi-heuristic origin, the value of the parameter γ being deduced from numerical simulations.

4. Comparison with some finite element micromechanical simulations

4.1. Koplik and Needleman's simulations (completed)

FE micromechanical simulations of void growth and coalescence have been performed by Koplik and Needleman (1988) for some cylindrical RVE with equal initial diameter and height, initially spherical voids, two values of the initial porosity ($f_0 = 0.0104$ and 0.0013, but only the first one will be considered here), and a sound matrix obeying an ideal-plastic behavior (as envisaged here). The loadings considered were

axisymmetric with predominant axial stress and the overall triaxiality was kept constant during the whole mechanical history. Since only medium and high triaxialities of 1, 2 and 3 were considered, we have completed these simulations by considering two lower triaxialities of 1/3 and 2/3. The computations were performed using the SYSTUS FE code developed by SYSTUS International. We shall now compare the results of these full numerical simulations with the predictions of the simplified, analytic model defined in the previous section. The theoretical value of $4/e \simeq 1.47$ derived by Perrin and Leblond (1990) for Tvergaard's (1981) parameter q_0 (for spherical cavities) will be adopted in the model predictions.

Fig. 3a–c exhibit the comparison for the normalized stress Σ_{eq}/σ_0 (where Σ_{eq} denotes the equivalent overall stress), the porosity and the void shape parameter. It can be seen on Fig. 3a that the model correctly reproduces the abrupt decrease of the stress during coalescence for triaxialities of 2/3, 1, 2 and 3. It also predicts absence of coalescence for a triaxiality of 1/3, just as the numerical simulation. Fig. 3b exhibits a remarkable agreement for the evolution of the porosity, including its rapid increase during coalescence for triaxialities of 2/3, 1, 2 and 3. Also, the model correctly predicts the stabilization of the porosity for a triaxiality of 1/3. This stabilization is obviously responsible for the absence of coalescence in that case. Its explanation is that for such a low triaxiality, which corresponds to some simple tension loading ($\Sigma_{zz} > \Sigma_{xx} = 0$), the initially spherical void quickly becomes quite prolate, so that its growth is no longer

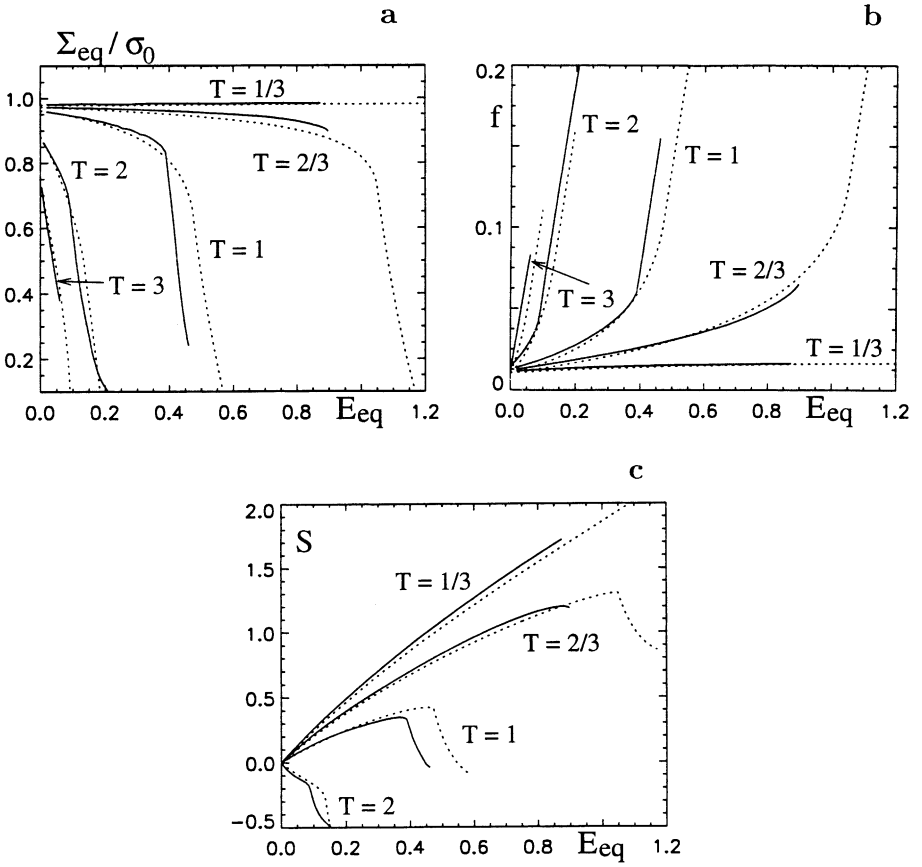

Fig. 3. Comparison of Koplik and Needleman's numerical results and ours (—) with model predictions (···): (a) normalized stress, (b) porosity, and (c) void shape parameter.

governed by the mean stress which is positive, but by the horizontal one which is zero; hence the void growth rate decreases. Finally, the evolution of the void shape parameter (Fig. 3c) is also correctly predicted by the model, including the evolution of the void toward oblate shapes even before coalescence for a triaxiality of 2. However, there is no great wonder here, since the evolution equations (29) and (33) for S prior and during coalescence were at least partially adjusted to match the numerical results.

Let us now show that two essential features of the model do lead to enhanced predictions. The first one is that the model accounts for the strain-induced anisotropy of the void distribution (through the consideration of three zones, sound, porous, sound) *even before coalescence*. The second one is that the model also accounts for void shape effects. It is easy to suppress the first feature of the model by simply ascribing, prior to coalescence, the value A (semi-height of the RVE) to the semi-height D of the porous zone; this zone indeed fills the entire RVE then, so that there are no longer three zones but a single one. The model thus obtained is quite, though not completely, similar to those of Pardoen and Hutchinson (2000) and Benzerga (2000). Fig. 4a–c, analogous to Fig. 3a–c, display the comparison between numerical results and predictions of the simplified model defined in that way. Comparison with Fig. 3a–c show that the improvement brought by the full model with respect to the simplified one is marginal for triaxialities of 1, 2 and 3. It is also unimportant for a triaxiality of $1/3$, for which no coalescence occurs. However, it is important for a triaxiality of $2/3$; indeed the simplified model predicts a notably overestimated ductility for that triaxiality, unlike the full one.

On the other hand, void shape effects can be disregarded by using Gurson's original model, instead of the GLD model, to describe the behavior of the central porous layer. In that case, we choose for D the value B (the radius of the RVE), in agreement with second term of Eq. (21) with $a = b$ (spherical cavity), and with Perrin's (1992) proposal. Fig. 5, analogous to Fig. 3a, shows the comparison, for the sole normalized stress, between numerical results and predictions of this new simplified model. The model now errs by underestimating the ductility for a triaxiality of $2/3$, and even more by predicting occurrence of coalescence for a triaxiality of $1/3$, in contradiction with the numerical simulation. The explanation of this erroneous prediction of occurrence of coalescence is that the simplified model disregarding void shape effects simply relates void growth to the mean stress (which is positive), whereas because of the prolate shapes resulting from the loading considered, it is in fact essentially governed by the lateral stress (which is zero); thus the simplified model overestimates void growth.

4.2. Sovik's simulations

Among the FE micromechanical simulations which have been performed by various authors, those of Sovik (1996) are of special interest because this author specifically studied the influence of initial void shape. Indeed he considered initial values of the ratio a/b $(= e^S)$ of $1/3$, $1/2$ (oblate voids), 1 (spherical void), 2 and 3 (prolate voids). On the other hand, he took equal values for the initial height and diameter of the RVE. The value of the initial porosity was smaller than in the work of Koplik and Needleman (1988), namely $f_0 = 0.0002$. A triaxiality of 1 was considered.

A higher value for Tvergaard's parameter q_0 than before, namely 1.6, was used in the model predictions, because of the very low value of the initial porosity. Indeed this value is compatible with accurate numerical studies of growth of a single void in an infinite matrix (zero porosity) performed by Huang (1991); see also the work of Gologanu et al. (1997). Fig. 6a and b show the comparison between Sovik's FE results and the model predictions, for the normalized stress and the porosity. The model can be observed to yield very good results which reproduce the strong dependence of ductility upon initial void shape (the more oblate the initial void, the lower the ductility, as one could expect). These comparisons thus again evidence the importance of incorporating void shape effects in predictive models of void coalescence, not only for low triaxialities but even for moderate ones of order unity.

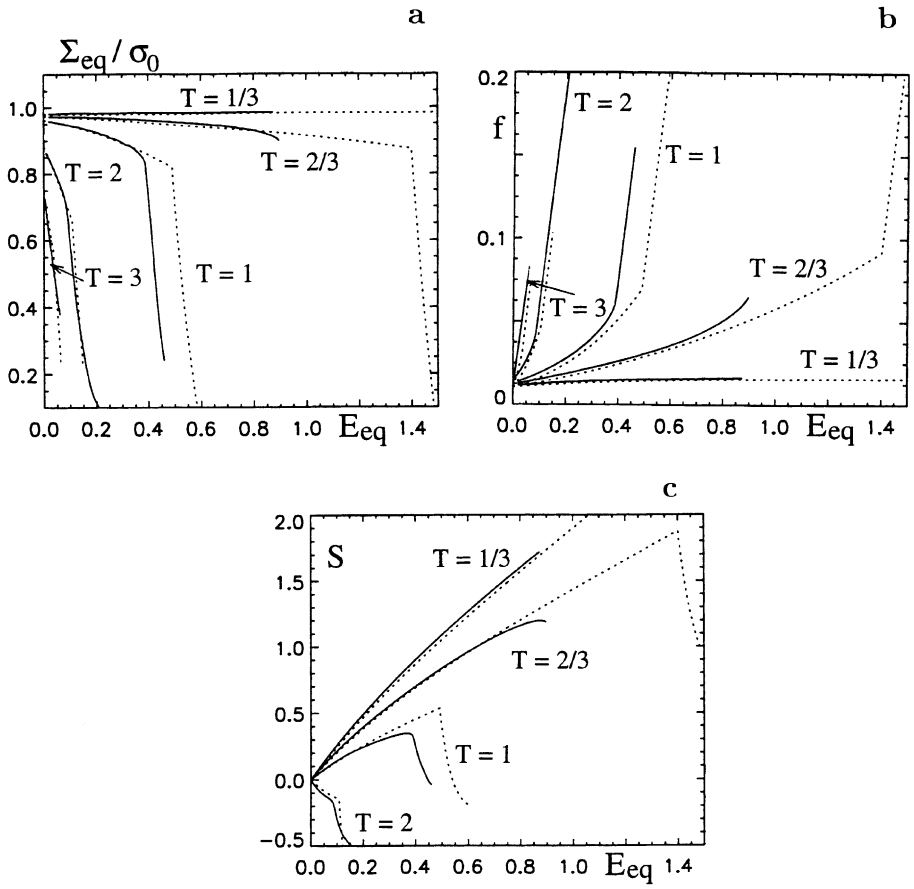

Fig. 4. Same as Fig. 3, but for the simplified model considering only one (porous) layer prior to coalescence.

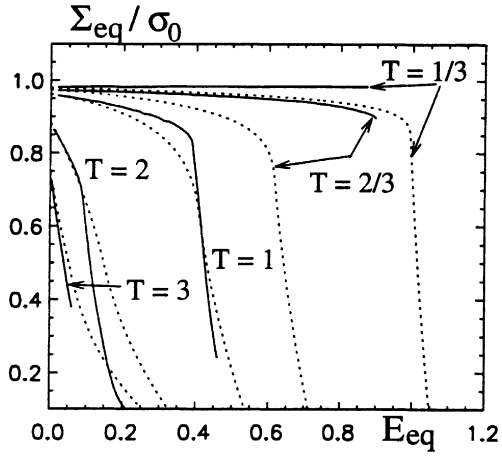

Fig. 5. Same as Fig. 3a, but for the simplified model using the Gurson model instead of the GLD model in the porous layer.

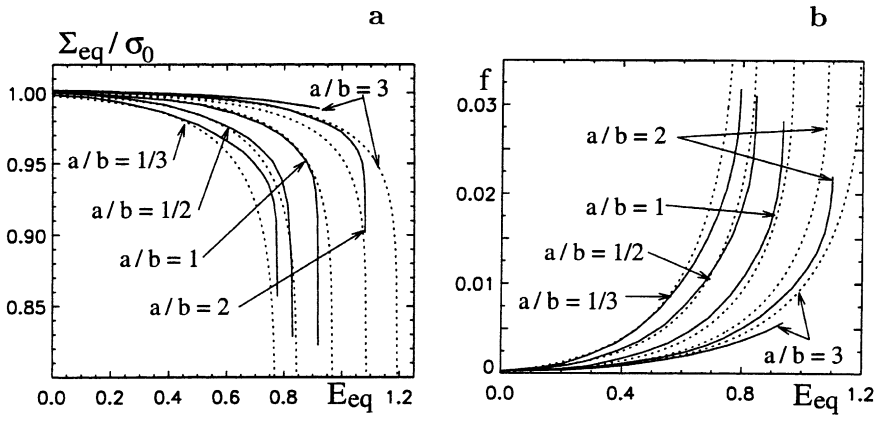

Fig. 6. Comparison of Sovik's numerical results (—) with model predictions (···): (a) normalized stress, and (b) porosity.

Appendix A.

The aim of this appendix is to discuss the difference between these expressions of the parameter h_T given by Eq. (19) and those proposed by Gologanu et al. (1997).

In view of the definition (1) of the void shape parameter S, there are two possible expressions for its time-derivative. The first one, which immediately derives from the definition, is

$$\dot{S} \equiv \frac{\dot{a}_1}{a_1} - \frac{\dot{b}_1}{b_1}. \tag{A.1}$$

This expression of $\dot{S}$ can be termed "pointwise", since it relates $\dot{S}$ to the motion of certain special points on the void surface. However, there is another, alternate expression of $\dot{S}$, namely

$$\dot{S} \equiv D_{zz}^{(v)} - D_{xx}^{(v)}, \tag{A.2}$$

where $\mathbf{D}^{(v)}$ denotes the overall strain rate of the void, which is defined as an integral over the void surface involving the velocity field. This is an expression "in mean value" of $\dot{S}$.

Of course, Eqs. (A.1) and (A.2) are equivalent if the void remains spheroidal during the mechanical history. Unfortunately, numerical simulations detailed in Gologanu's (1997) thesis show that such is only approximately the case in reality and that Eqs. (A.1) and (A.2) are in fact *not* equivalent. These numerical simulations lead to the following heuristic expressions of h_T:

$$h_T = \begin{cases} 1 - T^2 & \text{if } (\Sigma_{zz} - \Sigma_{xx})\mathrm{tr}\,\mathbf{\Sigma} > 0, \\ 1 - T^2/2 & \text{if } (\Sigma_{zz} - \Sigma_{xx})\mathrm{tr}\,\mathbf{\Sigma} < 0 \end{cases} \tag{A.3}$$

for the pointwise definition (A.1) of $\dot{S}$ and

$$h_T = \begin{cases} 1 - (T^2 + T^4)/9 & \text{if } (\Sigma_{zz} - \Sigma_{xx})\mathrm{tr}\,\mathbf{\Sigma} > 0, \\ 1 - (T^2 + T^4)/18 & \text{if } (\Sigma_{zz} - \Sigma_{xx})\mathrm{tr}\,\mathbf{\Sigma} < 0 \end{cases} \tag{A.4}$$

for the definition (A.2) in mean value.

In the work of Gologanu et al. (1997), the definition (A.2) in mean value and the associated expressions (A.4) were adopted. The motivation for this choice was that these formulae account better for the mean deformation of the void. However, in FE micromechanical simulations of the type presented in Section 4, it is customary to deduce the evolution of the shape parameter from that of the axes of the void. We therefore adopt this convention here, which leads us to prefer formulae (A.1) and (A.3).

References

Benzerga, A.A., 2000. Rupture ductile des tôles anisotropes. Thèse de Doctorat, Ecole Nationale Supérieure des Mines de Paris, Paris, France.

Brocks, W., Sun, D.Z., Hönig, A., 1995. Verification of the transferability of micromechanical parameters by cell model calculations with visco-plastic materials. Int. J. Plast. 11, 971–989.

Garajeu, M., 1995. Contribution à l'étude du comportement non linéaire de milieux poreux avec ou sans renfort. Thèse de Doctorat, Université de la Méditerranée, Marseille, France.

Gologanu, M., 1997. Etude de quelques problèmes de rupture ductile des métaux. Thèse de Doctorat, Université Pierre et Marie Curie, Paris, France.

Gologanu, M., Leblond, J.-B., Perrin, G., Devaux, J., 1997. Recent extensions of Gurson's model for porous ductile metals. In: Suquet, P. (Ed.), Continuum Micromechanics, CISM Courses and Lectures no 377. Springer, New York, pp. 61–130.

Gurson, A.L., 1977. Continuum theory of ductile rupture by void nucleation and growth. Part I: Yield criteria and flow rules for porous ductile media. ASME J. Engng. Mater. Technol. 99, 2–15.

Hom, C.L., McMeeking, R.M., 1989. Void growth in elastic–plastic materials. ASME J. Appl. Mech. 56, 309–317.

Huang, Y., 1991. Accurate dilatation rates for spherical voids in triaxial stress fields. ASME J. Appl. Mech. 58, 1084–1086.

Koplik, J., Needleman, A., 1988. Void growth and coalescence in porous plastic solids. Int. J. Solids Struct. 24, 835–853.

Kuna, M., Sun, D.Z., 1996. Three-dimensional cell model analyses of void growth in ductile materials. Int. J. Fract. 81, 235–258.

Pardoen, T., Delannay, F., 1998. The coalescence of voids in prestrained notched round copper bars. Fatigue Fract. Engng. Mater. Struct. 21, 1459–1472.

Pardoen, T., Hutchinson, J.W., 2000. An extended model for void growth and coalescence. J. Mech. Phys. Solids 48, 2467–2512.

Perrin, G., 1992. Contribution à l'étude théorique et numérique de la rupture ductile des métaux. Thèse de Doctorat, Ecole Polytechnique, Palaiseau, France.

Perrin, G., Leblond, J.-B., 1990. Analytical study of a hollow sphere made of plastic porous material and subjected to hydrostatic tension – application to some problems in ductile fracture of metals. Int. J. Plasticity 6, 677–699.

Richelsen, A.B., Tvergaard, V., 1994. Dilatant plasticity or upper bound estimates for porous ductile solids. Acta Metall. 42, 2561–2577.

Rudnicki, J.W., Rice, J.R., 1975. Conditions for the localization of deformation in pressure-sensitive dilatant materials. J. Mech. Phys. Solids 23, 371–394.

Sovik, O. P., 1996. Numerical modelling of ductile fracture – a damage mechanics approach. Ph.D. Thesis, Norwegian University of Sciences and Technology, Trondheim, Norway.

Thomason, P.F., 1985. Three-dimensional models for the plastic limit-loads at incipient failure of the intervoid matrix in ductile porous solids. Acta Metall. 33, 1079–1085.

Tvergaard, V., 1981. Influence of voids on shear band instabilities under plane strain conditions. Int. J. Fract. 17, 389–407.

Worswick, M.J., Pick, R.J., 1990. Void growth and constitutive softening in a periodically voided solid. J. Mech. Phys. Solids 38, 601–625.

Yamamoto, H., 1978. Conditions for shear localization in the ductile fracture of void containing materials. Int. J. Fract. 14, 347–365.